MR image denoising method for brain surface 3D modeling*

ZHAO De-xin (赵德新)**, **LIU Peng-jie** (刘朋杰), **and ZHANG De-gan** (张德干)
Tianjin Key Laboratory of Intelligent Computing & Novel Software Technology, Key Laboratory of Computer Vision and System, Ministry of Education, Tianjin University of Technology, Tianjin 300384, China

(Received 7 July 2014)

Three-dimensional (3D) modeling of medical images is a critical part of surgical simulation. In this paper, we focus on the magnetic resonance (MR) images denoising for brain modeling reconstruction, and exploit a practical solution. We attempt to remove the noise existing in the MR imaging signal and preserve the image characteristics. A wavelet-based adaptive curve shrinkage function is presented in spherical coordinates system. The comparative experiments show that the denoising method can preserve better image details and enhance the coefficients of contours. Using these denoised images, the brain 3D visualization is given through surface triangle mesh model, which demonstrates the effectiveness of the proposed method.

Document code: A **Article ID:** 1673-1905(2014)06-0477-4
DOI 10.1007/s11801-014-4105-8

The three-dimensional (3D) reconstruction of brain structures from magnetic resonance (MR) imaging is a crucial work in clinical diagnosis, surgical planning and the analysis of neuroanatomical variability. MR imaging is the most powerful imaging technique, and it can be adopted for brain imaging. MR images are affected by several noise sources, where the main source is thermal noise introduced by the movement of the charged particles in the radio frequency coils. These noises can affect the quality of the MR images and limit the correct diagnosis. Therefore, the denoising should be firstly performed to improve the image quality. Generally, post-processing filtering techniques are of high demand because these methods will not increase the acquisition time or reduce the spatial resolution compared with the acquisition stage filtering of MR imaging[1]. There are many kinds of denoising methods proposed in recent years, such as Wiener filtering[2], principal component analysis[3], non-local means[4] and wavelets analysis[5]. Wavelet has superior performance in image denoising due to the multi-resolution properties. Many techniques based on thresholding of wavelet coefficients are proposed for denoising, and the main idea is to transform the data into the wavelet basis. Wang[6] introduced a hyperbolic shrinkage function in the spherical coordinates (Sph-Wavelet), which avoids processing the wavelet coefficients directly. Khare[7] proposed an adaptive soft threshold function, which used multilevel adaptive thresholding and shrinkage (MATS) on complex wavelet coefficients. BiShrink method[8] used a bivariate shrinkage function which models the statistical dependence between a wavelet coefficient and its parent. This approach needs to estimate the marginal variance of the coefficient in a local neighborhood. All these methods attempt to extract the maximum amount of useful information from data, they are subject to some assumptions, so these methods may perform different effects in terms of denoising quality, computation cost and boundary preserving.

In this paper, using spherical transform into wavelet domain, we present an improved nonlinear shrinkage function for suppressing the Gaussian white noise in MR imaging. This idea is to process the radial component instead of the wavelet coefficients, because the radial direction in spherical coordinate carries the most energy of noise in high frequency. We compare our method with other three image denoising methods in peak signal noise ratio (PSNR) and mean square error (MSE), and the results are satisfactory in denoising quality. From a set of parallel slices generated from MR imaging, it is possible to reconstruct and display the external surface of brain using the triangle meshes of the geometric modeling. The results of 3D triangle mesh generation and visualization for MR brain slices are given.

We focus on the MR image denoising and attempt to remove the noise exsisting in the MR imaging signal and preserve the image characteristics. The raw and complex MR data acquired in the Fourier domain are characterized by a zero mean Gaussian probability density function,

* This work has been supported by the National Natural Science Foundation of China (No.61202169), the Tianjin Key Natural Science Foundation (No.13JCZDJC34600), the China Scholarship Council (CSC) Foundation (No.201308120010), and the Training Plan of Tianjin University Innovation Team (No.TD12-5016).
** E-mail: qiqiharxin@163.com

and the noise distributions in the real and imaginary components will be still Gaussian after the inverse Fourier transform[9]. So the noise in MR imaging data is well modeled by a Gaussian probability density function. The noise estimation methods in wavelet domain are the most popular among the effective denoising procedures. In fact, wavelets have been used for denoising in many medical imaging applications[10,11]. The image in wavelet domain is decomposed into approximation sub-band and detail sub-band in various scales.

The basic idea of wavelet denoising is as follows. Firstly, calculate the discrete wavelet transform, then remove noise from the wavelet coefficients, and finally apply the inverse wavelet transform to reconstruct a denoised signal. The detailed coefficients are regarded as soft or hard threshold to estimate the signal components. Wavelet shrinkage is a non-linear process. It mostly depends on the threshold parameters which have much influence on denoising quality. Assume that an additive noise model in each wavelet sub-band is

$$w_k = x_k + n_k, \tag{1}$$

where w_k is the wavelet coefficient, x_k is the unknown noise-free signal component, and n_k is the noise contribution. The wavelet shrinkage estimators are often represented as

$$\hat{x}_k = P_k w_k, \quad 0 \le P_k \le 1, \tag{2}$$

where P_k denotes a shrinkage factor. So w_k is likely to represent pure noise as P_k close to 0, while w_k is likely to represent noise-free image as P_k close to 1. There are two classical thresholding rules, in which a threshold value T is defined and P_k is specified as follows. For the hard thresholding,

$$P_k = \begin{cases} 1 & |w_k| \ge T \\ 0 & |w_k| < T \end{cases}, \tag{3}$$

and for the soft thresholding,

$$P_k = \begin{cases} 1 - T/|w_k| & |w_k| \ge T \\ 0 & |w_k| < T \end{cases}. \tag{4}$$

So the critical task in wavelet thresholding is the threshold selection.

Zhang et al[12-14] redefined the spherical transform in wavelet domain. If f denotes a two-dimensional image, and $C_{j,k}^{(i)}$ (i=1,2,3) are the wavelet decomposing high frequency components of the image f, the spherical transform in wavelet is defined as

$$\begin{cases} R = \sqrt{\left(C_{j,k}^{(1)}\right)^2 + \left(C_{j,k}^{(2)}\right)^2 + \left(C_{j,k}^{(3)}\right)^2} \\ \theta = \mathrm{tg}^{-1}\left(C_{j,k}^{(2)} / C_{j,k}^{(1)}\right) \\ \varphi = \cos^{-1}\left[C_{j,k}^{(3)} \Big/ \sqrt{\left(C_{j,k}^{(1)}\right)^2 + \left(C_{j,k}^{(2)}\right)^2 + \left(C_{j,k}^{(3)}\right)^2}\right] \end{cases}, \tag{5}$$

where $C_{j,k}^{(1)}$, $C_{j,k}^{(2)}$ and $C_{j,k}^{(3)}$ represent horizontal, vertical and diagonal components, respectively, R is the radial component in spherical coordinate system, and θ and φ are the phase angle components. The advantage of introducing spherical coordinate to wavelet domain is that the image energy in the three high frequency parts can be completely mapped to the radial component R. Then, we just need to process the radial component R instead of the wavelet coefficients, which can reduce the image distortion in a certain degree. Furthermore, Zhang[15] proposed a new adaptive threshold $T = \sqrt{6}|R|/N$, where N is image pixel, which has been proved based on Besov space norm theory.

In this paper, keeping focus on MR image denoising, we apply the threshold to a new shrinkage function as

$$R^*(i,j) = \begin{cases} R(i,j) - \dfrac{T}{1+\log[1+R(i,j)-T]} & R(i,j) > T \\ 0 & R(i,j) \le T \end{cases}, \tag{6}$$

which has much benefit to the MR images.

We can see that the constructed shrinkage function continues at T, because $R^*(i,j)=0$ when $R(i,j)\le T$. If $R(i,j)>T$, the proposed function $R^*(i,j)$ satisfies the following inequation as

$$R(i,j) - T < R^*(i,j) < R(i,j). \tag{7}$$

Therefore, the proposed shrinkage function curve is located between the traditional hard threshold and soft threshold.

The procedure of the proposed denoising method is as follows. (I) Decompose the observed image f by wavelet transform at different levels; (II) Transform the high frequency coefficients of $C_{j,k}^{(i)}$ (i=1,2,3) at different scales to spherical coordinates system by Eq.(5); (III) Process the radial component R using the proposed curve shrinkage function of Eq.(7) if the estimated radial component satisfies $R^*(i,j)=0$, then set the angles of θ and φ to zero; (IV) Do inverse spherical transform to R^*, θ and φ in spherical coordinates as follows,

$$\begin{cases} (C_{j,k}^{(1)})^* = R^* \sin\varphi\cos\theta \\ (C_{j,k}^{(2)})^* = R^* \sin\varphi\cos\theta \\ (C_{j,k}^{(3)})^* = R^* \cos\varphi \end{cases}, \tag{8}$$

where $(C_{j,k}^{(1)})^*$, $(C_{j,k}^{(2)})^*$ and $(C_{j,k}^{(3)})^*$ are the estimated horizontal, vertical and diagonal high frequency components, respectively; (V) Reconstruct the image by applying the inverse wavelet transform.

A series of experiments based on real MR images are done to evaluate the proposed denoising shrinkage function and the 3D triangulation mesh model. We got the MR images from Tianjin First Center Hospital in China, including 51 head tomography slices of one person, where the image size of each slice is 128×128.

It is a popular way to evaluate the denoising effects using the PSNR and MSE, which are expressed as

$$PSNR = 10 \times \log_{10}\left[\frac{(2^n - 1)^2}{MSE}\right], \tag{9}$$

$$MSE = \frac{1}{MN}\sum_{i,j}^{M,N}(f_{i,j} - f_{i,j}^*)^2, \tag{10}$$

where $f_{i,j}$ is the original image, $f_{i,j}^*$ is the image after removing noise, and M and N are the sizes of the images.

The main source of noise in MR images is the thermal noise in the patient. The signal component of the measurements is achieved in both real and imaginary channels, and each of the two orthogonal channels is affected by additive white Gaussian noise. The noise in the reconstructed complex-valued data is thus complex white Gaussian noise. So by adding white Gaussian noise to the MR images, we get PSNR and MSE at different decomposition levels as shown in Fig.1. It can be seen from Fig.1 that the denoising effect tends to be stable in decomposition levels of 3, 4 and 5. When the decomposition level is greater than 6, the turbulence will generate in PSNR and MSE.

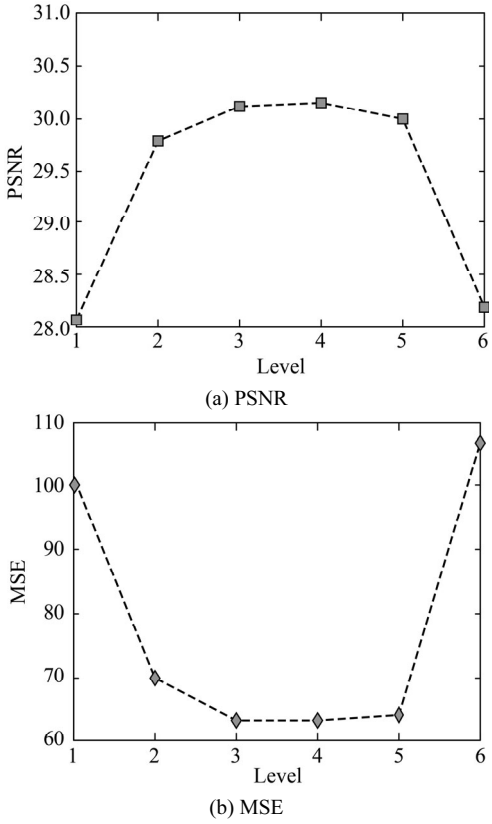

Fig.1 PSNR and MSE on decomposition level

We choose level 4 as decomposition scale in the next experiments. In order to compare the effects of different denoising methods, we add white Gaussian noise to the original image, and compare our method with other three denoising algorithms of SphWavelet[6], MATS[7] and BiShrink[8]. Fig.2 shows the denoising results of four methods on MR image. Fig.2(a) is the original MR image which is the 24th of the head MR image sequence, Fig.2(b) is the image with an increasing white Gaussian noise when the mean and deviation of the noise are 0 and 25, respectively, Fig.2(c)–(e) are the results of SphWavelet method, MATS method and BiShrink algorithm, respectively, and Fig.2(f) is the result of the shrinkage function we proposed. Compared with these denoising algorithms, our proposed method shows the satisfactory result.

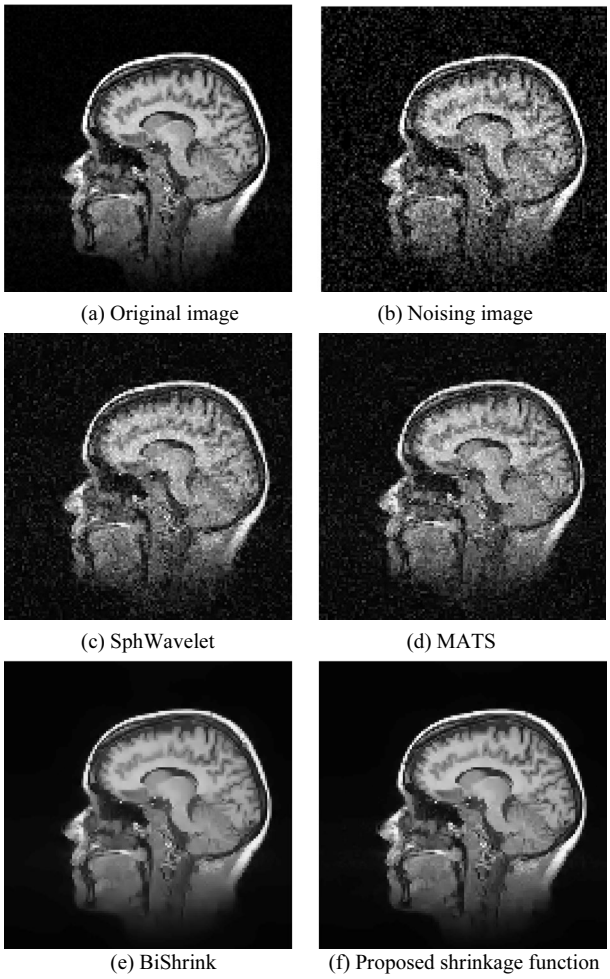

Fig.2 Comparison of results by four kinds of denoising methods on the MR image

We evaluate the validity of the proposed method by computing PSNR and MSE. After adding Gaussian white noise with different deviations, the results are shown in Fig.3. From PSNRs of four methods shown in Fig.3(a), we can see our method can get the highest PSNR in each noise deviation. From Fig.3(b), we can see that our method can get the lowest MSE in each deviation. These data prove the satisfactory result of the shrinkage function.

We segment brain from the denoised MR imaging head slices, using triangle mesh algorithm for MR imaging 3D

surface reconstruction, and the brain mesh result is shown in Fig.4. The presented result demonstrates the effectiveness of the brain reconstruction.

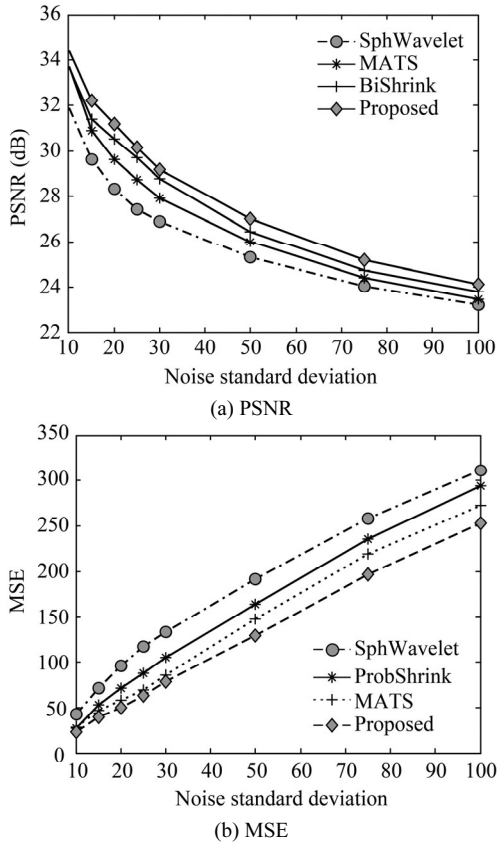

Fig.3 PSNR and MSE results of four kinds of denoising methods

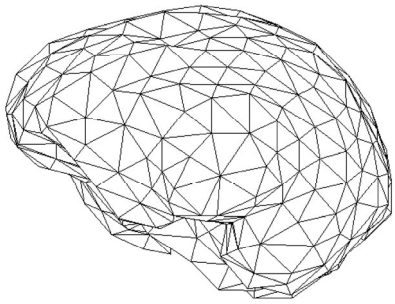

Fig.4 Brain mesh result

Denoising is the first and necessary step to be taken before the image data are analyzed. It is difficult to remove the noise from MR images, and the state-of-art methods vary from standard filters to more advanced filters. We present a method for denoising MR images based on curve shrinkage function in the spherical coordinates, and it has the advantage that the most energy of noise is carried by the radial component, so we can focus on processing the radial component instead of the wavelet coefficients in other nonlinear threshold filtering methods. The experiments show that it is effective on terms of improving PSNR as well as preserving the features of the activated region. The running time of the proposed denoising method is less than that of the compared algorithms, and it is more obvious with the increase of scale. However, if the noise in MR image with low signal-to-noise ratio is strictly Rician-distributed, this can be no longer approximated as white Gaussian like that in the classical methods. Our further study will pay more attention to the Rician noise removal in MR images.

References

[1] C. Shyam Anand and Jyotinder S. Sahambi, Magnetic Resonance Imaging **28**, 842 (2010).

[2] Mohan J., Krishnaveni V. and Guo Y., Biomedical Signal Processing and Control **8**, 779 (2013).

[3] Chen G. and Qian S. E., IEEE Transactions on Geoscience and Remote Sensing **49**, 973 (2011).

[4] José V. Manjón, Pierrick Coupé, Luis Martí‐Bonmatí, D. Louis Collins and Montserrat Robles, Journal of Magnetic Resonance Imaging **31**, 192 (2010).

[5] Ruikar S. D. and Doye D. D., International Journal of Advanced Computer Science and Applications **2**, 49 (2011).

[6] Wang Shengqian, Zhou Yuanhua and Zou Daowen, Journal of Infrared and Millimeter Waves **20**, 387 (2001). (in Chinese)

[7] Khare A., Tiwary U. S. and Pedrycz W., Imaging Science Journal **58**, 340 (2010).

[8] Sendur L. and Selesnick I. W., IEEE Signal Processing Letters **9**, 438 (2002).

[9] Jeny Rajan, Dirk Poot, Jaber Juntu and Jan Sijbers, Physics in Medicine and Biology **55**, 441 (2010).

[10] Florian Luisier, Cedric Vonesch, Thierry Blu and Michael Unser, Signal Processing **90**, 415 (2010).

[11] Ashish Khare, Manish Khare and Yongyeon Jeong, Signal Processing **90**, 428 (2010).

[12] Degan Zhang and Xiaodan Zhang, Enterprise Information Systems **6**, 473 (2012).

[13] Degan Zhang, Guang Li and Ke Zheng, IEEE Transaction on Industrial Informatics **10**, 766 (2014).

[14] Degan Zhang and Xuejing Kang, Journal on Advances in Signal Processing **110**, 1 (2012).

[15] Zhang De-Gan, Kang Xue-Jing and Wang Dong, Journal of Optoelectronics·Laser **23**, 180 (2012). (in Chinese)